Peculiarities of ball-milling induced crystalline-amorphous transformation in Cu-Zr–Al-Ni-Ti alloys

K.Tomolya[1], D.Janovszky[1a], A.Sycheva[1], M.Sveda[1], T.Ferenczi[2], A.Roósz[1]
[1]MTA-ME Materials Science Research Group, Miskolc, Hungary
[2]University of Miskolc, Miskolc, Hungary
[a]**Corresponding author:** fekjd@uni-miskolc.hu

Abstract
An amorphization process in $(Cu_{49}Zr_{45-x}Al_{6+x})_{100-y-z}Ni_yTi_z$ (x=1, y,z=0;5;10) induced by ball-milling is reported in the present work. The aim was investigation of the effect of Ni and Ti addition to $Cu_{49}Zr_{45}Al_6$ and $Cu_{49}Zr_{44}Al_7$ based alloys as well as type of initial phases on the amorphization processes. Also the milling time sufficient for obtaining fully amorphous state was determined. The entire milling process lasted 25 hours. Drastic structural changes were observed in each alloy after first 5 h of milling. In most cases, after 15 h of milling the powders had fully amorphous structure according to XRD except for those ones, where TEM revealed a few nanosized crystalline particles in the amorphous matrix. In $(Cu_{49}Zr_{45}Al_6)_{80}Ni_{10}Ti_{10}$ alloy the amorphization process took place after 12 h of milling and the amorphous state was stable up to 25 h of milling. In the case of $(Cu_{49}Zr_{44}Al_7)_{80}Ni_{10}Ti_{10}$ alloy the powders have fully amorphous structure between 12 h and 15 h of milling.

Keywords: amorphous powder**,** Cu-Zr-Al alloy, ball-milling, microstructure

1. Introduction

It is well known that industry expects development of new stronger and lighter materials from materials science. So bulk metallic glasses (BMGs) have been extensively studied nowadays. Despite excellent mechanical properties of BMGs, the high-volume industrial application has not yet become a reality. Production of BMGs with greater than 1 dm in size is not solved; only some Pt and Pd-based alloys and Zr-based [1-2], Cu-based [3-4] and Ti-based [5-6] BMGs have been produced with few cm sizes only. The powder metallurgy (PM) can solve this problem via consolidation of amorphous powders [7-9]. The first step of PM is manufacturing amorphous powders by high-pressure gas atomization or by solid state techniques, e.g. high energy ball-milling. Recently, Cu-Zr based BMGs [10-11] have attracted great attention due to high strength and high thermal stability against crystallization with lower costs than Zr-based BMGs. Cu-Zr-Al BMGs [12-16] have such advantageous properties as good toughness indicated by their high Charpy impact value, good corrosion resistance, and high glass forming ability (GFA). However, their plasticity at room temperature is usually less than 2 % compared with that of BMGs in the Zr–Ni–Al and Zr–Al–Ni–Cu systems [17-18]. Ni and Ti form a complete solid solution with Cu and Zr. In the Cu-Zr-Al-Ni-Ti system, the heat of mixing between elements is negative; only in the case of Ni-Cu (ΔH_{mix} = 4 kJ/mol [19]) it is positive. In the Cu-Zr-Al system, two compositions with high glass forming ability [20] were selected as basic alloy ($Cu_{49}Zr_{45}Al_6$ and $Cu_{49}Zr_{44}Al_7$) and Ni and Ti were added as alloying elements.
In this work, the structure evolution of alloyed $(Cu_{49}Zr_{45-x}Al_{6+x})_{100-y-z}Ni_yTi_z$ (x=1, y,z=0;5;10) powders was investigated. The aim of the present work is to create alloys in this composition system with fully amorphous structure via high energy ball-milling. It is well known that the progress of amorphization reaction is a recycling process (crystalline-amorphous-crystalline).

Furthermore, it is important to determine the milling time, which is sufficient to obtain the fully amorphous state.

2. Experimental procedure

Master alloy ingots were prepared by arc melting the mixtures of Cu, Zr, Al, Ni, Ti pure metals (min. 99.99%) under purified argon atmosphere. The chemical compositions of master alloys can be seen in Table 1. The master alloys were grinded and fractioned to a particle size below 300 μm for ball-milling. The mechanical milling was performed in a Pulverisette 5 high-energy ball-mill in argon atmosphere using stainless steel vial and balls. The maximal milling process lasted 25 h in order to assure that the milling has proceeded long enough for the samples to reach the amorphous state, but short enough to avoid excessive contamination from the milling media. The milling process was interrupted every hour. Each interruption was followed by a period of 2 hours to cool down the vials. The milled powder samples were extracted every 5 hours in order to examine the progress of amorphization reaction. In order to analyze the microstructure, both the master alloys and the powders were embedded in acrylic resin, then polished and etched with 0.5 % hydrofluoric acid for 5 sec. The structure of both master alloy ingots and both powders was investigated by a Hitachi S4800 Field Emission Scanning Electron Microscope (SEM) equipped with a Bruker AXS Energy-dispersive X-ray Spectrometer (EDS) system, a FEI Technai G2 Transmission Electron Microscope (TEM) and a Philips PW 1830 X-ray diffractometer (XRD) with monochromatized CuKα radiation with a wavelength of 0.15418 nm using an anode voltage of 40 kV and a current of 305 mA. Amorphous fraction was determined by evaluation of XRD patterns. Using a combination of free software named Fityk 0.98 and software developed by us and called GerKiDo, different curves can be fitted to selected measuring points. The amorphous fraction can be calculated after measuring the area under the curves. Details are shown in Ref. 21. Thermal analysis was performed by a Netzsch 204 Differential Scanning Calorimeter (DSC) with a heating rate of 0.67 K/s.

3. Results and discussion

3.1. Initial microstructure of master alloys

Fig. 1 presents the microstructure of master alloys. Based on the SEM, TEM analysis, results of EDAX and XRD analysis (Fig. 2), the phases formed in the master alloys have been identified. In the case of 1Alloy0-0 two phases solidified as primary phases from the liquid. It cannot occur under equilibrium conditions except for solidification of an alloy with eutectic composition. Monoclinic CuZr dendritic phase (a_0 = 3.4 Å, b_0 = 4.3 Å, c_0 = 5.6 Å, β = 106°) and an unknown phase with $Al_{13}Cu_{37}Zr_{50}$ composition solidified as primary phases (Figs. 1a, 2a). $Al_{13}Cu_{37}Zr_{50}$ has a distorted cubic unit cell with a_0 = 12.18 Å, γ = 90° as was mentioned in Ref. 22. This unknown phase has been already mentioned in literature [23] with the following composition 37.8 ± 1.8 at.% Cu, 49.2 ± 1.6 at.% Zr and 13.0 ± 0.4 at.% Al. CuZr and $AlCu_2Zr$ formed a fine eutectic. Owing to the addition of 5 at% Ni and Ti to the alloy 1Alloy5-5, massive CuZr(NiTi) dendritic phase solidified as primary phase in the master alloy (Figs. 1b, 2b). This phase dissolved 20 at% of Ti and 6 at% of Ni. $Cu_{10}Zr_7$(Ni) phase appeared in addition to CuZr. $Cu_{10}Zr_7$(Ni) phase dissolved 15-25 at% of Ni. CuZr(NiTi), $Cu_{10}Zr_7$(Ni) and $AlCu_2Zr$ phases formed fine ternary eutectic. In the 1Alloy10-10 the big dendrites were CuZr(NiTi) phase (Figs. 1c, 2c). The lattice parameters of CuZr reduced due to the dissolved Ni and Ti: a_0 = 3.2 Å, b_0 =4.1 Å, c_0 = 5.4 Å, β = 106°. In this case four phases formed the eutectic: CuZr(NiTi), $Cu_{10}Zr_7$(Ni), $Al_{13}Cu_{37}Zr_{50}$ and a new phase. $Al_{13}Cu_{37}Zr_{50}$ solidified as

100-200 nm grains. A hexagonal Laves Cu_2ZrTi type phase [24] was the new phase in this alloy with $a_0 = 5.3$ Å, $c_0 = 8.9$ Å. The average grain size is about a few hundred nm.

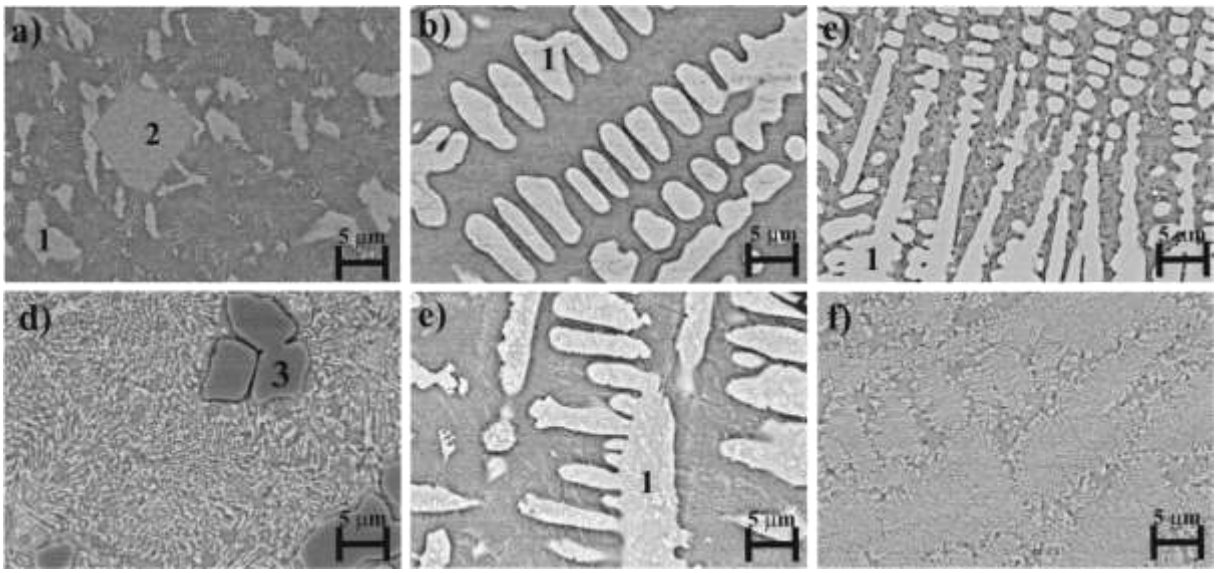

Fig.1: Microstructure of master alloys; a) 1Alloy0-0, b) 1Alloy5-5, c) 1Alloy10-10, d) 2Alloy0-0, e) 2Alloy5-5, f) 2Alloy10-10: 1 – CuZr, 2 – $Al_{13}Cu_{37}Zr_{50}$, 3 – $AlCu_2Zr$

Although the nominal compositions are very similar in the two basic alloys 1Alloy0-0 and 2Alloy0-0, the solidified phases are different. This phenomenon can be explained by the fact that these two compositions are close to the eutectic valley based on the calculated Al-Cu-Zr ternary diagram [25]. In 2Alloy0-0 $AlCu_2Zr$ solidified as primary phase (Figs. 1d, 2d). In addition, CuZr and $Cu_{10}Zr_7$ were identified in this alloy. $AlCu_2Zr$, $Cu_{10}Zr_7$ and CuZr phases formed the ternary eutectic. In 2Alloy5-5 solidification started with large dendrites of the CuZr(NiTi) phase (Figs. 1e, 2e). This phase dissolved Ni and Ti similarly to CuZr(NiTi) in the case of 1Alloy5-5. Besides the CuZr(NiTi) phase, $Cu_{10}Zr_7$(Ni), $Al_{13}Cu_{37}Zr_{50}$ and Cu_2ZrTi type phases were identified in the fine eutectic. In 2Alloy10-10 alloy primary phase was not formed; eutectic structure has been obtained during solidification process (Fig. 1f). Four phases have been revealed in the eutectic structure: CuZr(NiTi), $Cu_{10}Zr_7$(Ni), $Al_{13}Cu_{37}Zr_{50}$ and Cu_2ZrTi type phase (Fig. 2f).

3.2. Microstructure evolution during different-time ball milling

The structure evolution of powders occurred during ball-milling was investigated as function of milling time, which can be seen in Fig. 2. Considering the XRD curves it can be concluded that drastic changes took place in each alloy after 5 h milling time. The diffraction peaks belonging to the crystalline phases reduced significantly after 5 h of milling. Monoclinic CuZr phase remained in the 1Alloy system based on the XRD analysis after 5 h of milling and in the case of 1Alloy0-0 a small amount of $AlCu_2Zr$ was found as well. Among the present phases CuZr was the most stable one. After 15 h of milling only a broad diffuse halo remained indicating fully amorphous structure in the case of 1Alloy0-0 and 1Alloy5-5 (Figs. 2 a-b).

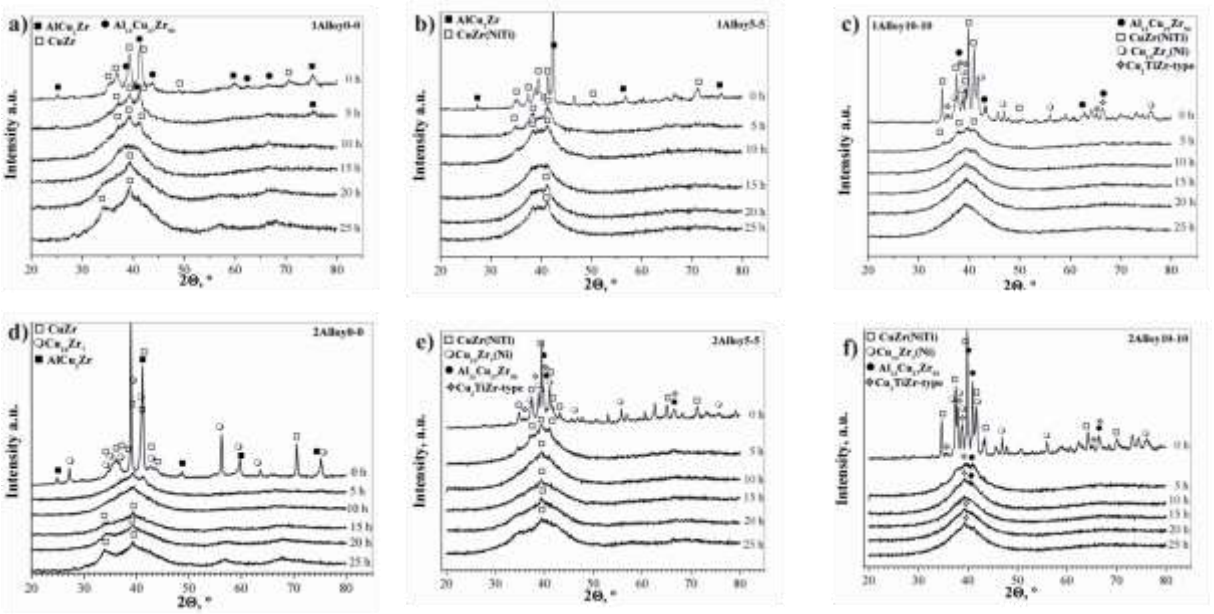

Fig. 2: XRD patterns of a) 1Alloy0-0, b) 1Alloy5-5, c) 1Alloy10-10, d) 2Alloy0-0, e) 2Alloy5-5, f) 2Alloy10-10 master alloys and as-milled powders.

TEM investigation revealed that CuZr phases embedded in the contrastless amorphous matrix in 1Alloy0-0 and 1Alloy 5-5 (Figs. 3 a-b). The monoclinic CuZr particles have a size of a few hundred nanometers in 1Alloy 0-0 and few tens of nanometers in 1Alloy5-5. The selected area electron diffraction (SAED) patterns recorded on areas of the matrix showed diffuse rings and discrete reflections (Figs. 3 a, b inset), which proves the presence of amorphous and also nanocrystalline parts in the matrix. Sharp diffraction peaks in the XRD pattern (Figs. 2 a, b) corresponding to CuZr phase appeared after 15 h of milling, which means that this phase formed from the metallic glass matrix. Milling process induced crystallization of CuZr phase in 1Alloy 0-0 and 1Alloy 5-5. The intensity and number of peaks in the XRD pattern belonging to CuZr increase slightly by further milling. According to the present experimental results, amorphous phase cannot be formed completely if the time is more than 15 h, amorphous phase transforms again into crystalline one. If shorter time is applied, amorphous phase cannot be formed completely based on the TEM investigation.

In the case of 1Alloy10-10 the difference in the XRD patterns was barely noticeable between 10 h and posterior milling times; a broad diffuse halo without sharp diffraction peaks can be seen. TEM examination confirmed the presence of an amorphous structure. SAED pattern of this composition after 15 h of milling showed only diffuse rings (Fig. 3c inset) featuring that the structure was fully amorphous. Between 10 and 15 h of milling samples were analyzed every hour in order to clarify the structural changes during mechanical milling. The XRD analysis showed that this alloy achieved amorphous structure after 12 h of milling.

In the case of 2Alloy 0-0 the process of structural changes was similar to 1Alloy 0-0. After milling for 10 h the alloy had amorphous structure according to XRD analysis (Fig. 2d). After 15 h milling time the diffraction peak of CuZr phase appeared again and increased slightly due to further milling. These results are in agreement with the TEM analysis. In Fig. 3d dark nanoparticles with a size of 1-20 nm embedded in the amorphous matrix are seen after 15 h milling. In the XRD pattern of 2Alloy 5-5 the monoclinic CuZr(NiTi) phase can be detected in the course of entire milling process ranging from 5 to 25 h (Fig. 2e). This indicates high stability of the monoclinic CuZr(NiTi) phase against milling.

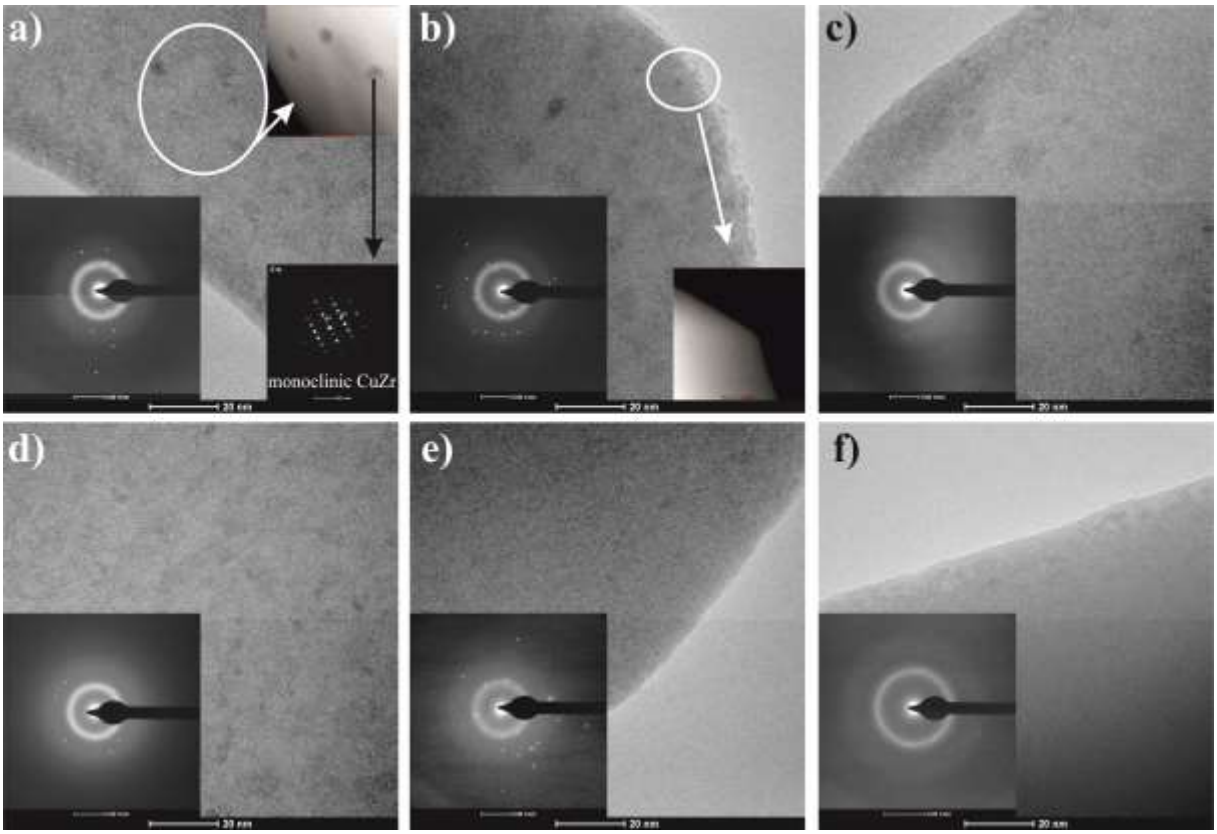

Fig. 3: Bright-field images and corresponding SAED patterns of different composition alloys after 15 h of milling, a) 1Alloy0-0, b) 1Alloy5-5, c) 1Alloy10-10, d) 2Alloy0-0, e) 2alloy5-5, f) 2Alloy10-10

The microstructure evolution of 2Alloy10-10 differs from the previous composition. The diffraction peaks of $Al_{13}Cu_{37}Zr_{50}$ and Cu_2ZrTi type phase were identified already after 10 h of milling (Fig. 2f). The full amorphous state was obtained after 15 h of milling based on the XRD and TEM analysis (Fig. 2, 3f). Further milling process induced crystallization of Cu_2ZrTi type phase (Fig. 2f). So due to the addition of 10 at% Ni and Ti the Cu_2ZrTi type phase is more stable against milling than CuZr phase.

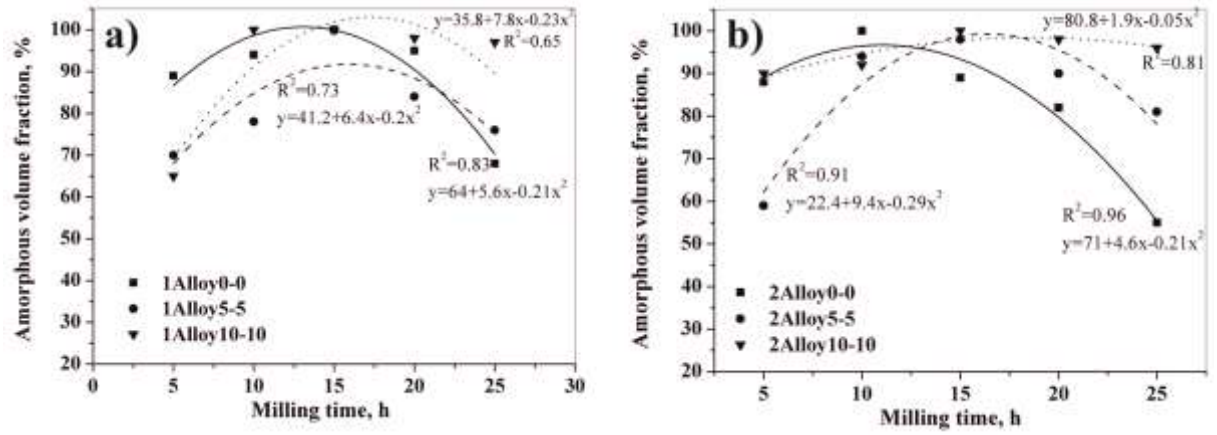

Fig.4: Correlation between milling time and amorphous fraction measured by XRD

Summarizing the present experimental results, it can be said that a close correlation was observed between the amorphous volume fractions and milling time (Fig. 4) based on the XRD analysis. The data obtained could be described by a parabolic relationship. It can be

seen that the crystalline-amorphous-crystalline process occurs in a relatively short milling time in the case of 1-2Alloy0-0 and 1-2Alloy5-5: the maximum volume fraction is achieved at 15 h and 10 h, respectively. For the 1-2Alloy10-10 the amorphous structure is more stable since the amorphous volume fraction does not decrease significantly even after 25 h milling time.

4. Conclusions

$Cu_{49}Zr_{45}Al_6$ and $Cu_{49}Zr_{44}Al_7$ compositions were selected as basic alloys and the effect of Ni and Ti as alloying elements was investigated on the amorphization process by ball-milling. Drastic changes took place in each alloy after 5 h milling time. The initial structure of the powders (before milling), the size, type and the quantity of phases and their influence on the amorphization process have been examined as well. The CuZr phase has high stability against milling in 1Alloy0-0 and 2Alloy0-0. This phase can absorb most of transmitted mechanical energy without formation of an amorphous structure. It is worth to mention that this phase can crystallize easily from amorphous state compared to the other phases in this system. In most cases, after 15 h of milling the powders had fully amorphous structure according to XRD except for those ones, where TEM revealed a few nanosized crystalline particles in the amorphous matrix. Furthermore, in the compositions alloyed with 5 at% of Ni and 5 at% of Ti CuZr phase can be observed as well which dissolved these alloying elements. 2Alloy5-5 could not be amorphized in the course of entire milling process lasted for 25 h. In 1Alloy10-10 the amorhization process took place differently owing to the higher amount of alloying elements. The phases including CuZr(Ni,Ti) disappeared after 12 h of milling and the amorphous state was stable up to 25 h of milling. 2Alloy10-10 has a eutectic structure which formed by CuZr(NiTi), $Cu_{10}Zr_7$(Ni), $Al_{13}Cu_{37}Zr_{50}$ and Cu_2ZrTi type phases. In this alloy Cu_2ZrTi type phase is the most stable since it disappears last and crystallizes first from the amorphous phase during milling. It is recommended to add 10 at% of Ni and 10 at% of Ti to both alloys in order to achieve fully amorphous structure after 12 h of ball-milling.

Acknowledgements

This work has been carried out as part of the TÁMOP 4.2.4.A/2-11-1-2012-0001 project within the framework of the New Hungarian Development Plan. The realization of this project is supported by the European Union, co-financed by the European Social Fund. The research work was carried out as part of the OTKA K 112623 project, as well.
The authors wish to thank Dr. Ildiko Cora and Peter Pekker (MTA-ME Materials Science Research Group) for TEM analysis of the samples. Special thanks goes to Dr. Marton Benke (Institute of Physical Metallurgy, Metal Forming and Nanotechnology, University of Miskolc) for XRD measurements.

References

[1] Y. Yue, R. Wang, D.Q. Ma, J.F. Tian, X.Y. Zhang, Q. Jing, M.Z. Ma, R.P. Liu, Intermetallics 2015; 60: 86
[2] C. Fan, C.T. Liu, G. Chen, G. Chen, D. Chen, X. Yang, P.K. Liaw, H.G. Yan, Intermetallics 38 (2013) 19-22
[3] P.W.B. Marques, J.M. Chaves, P.S. Silva Jr., O. Florencio, A. Moreno-Gobbi, L.C.R. Aliaga, W.J. Botta, J. Alloys Compd. 621 (2015) 319-323
[4] E.S. Park, H.J. Chang, D.H. Kim, J. Alloys Compd. 504S (2010) S27-S30

[5] Y.S. Wang a, b, G.J. Hao a, R. Ma a, Y. Zhang a, J.P. Lin a, *, Z.H. Wang c, J.W. Qiao Intermetallics 60 (2015) 66e71
[6] P. Gong, X. Wang, Y. Shao, N. Chen, X. Liu, K.F. Yao Intermetallics 43 (2013) 177e181
[7] J. Dutkiewicz, L. Jaworska, W. Maziarz, T. Czeppe, M. Lejkowska, M. Kubicek, M. Pastrnak, J. Alloys Compd. 434-435 (2007) 333-335
[8] H.-M. Lin, Y.-W. Lin, P.-Y. Lee, J. Mater Sci (2008) 43:3118-312
[9] N. Yodoshi, R. Yamada, A. Kawasaki, A. Makino, J. Alloys Compd. 615 (2014) S61-S66
[10] X. Cui, F.Q. Zu*, Z.Z. Wang, Z.Y. Huang, X.Y. Li, L.F. Wang Intermetallics 36 (2013) 21e24
[11] X. Cui, F.Q. Zu*, Z.Z. Wang, Z.Y. Huang, X.Y. Li, L.F. Wang Intermetallics 36 (2013) 21e24
[12] Henry Kozachkov a, Joanna Kolodziejska a, William L. Johnson a, Douglas C. Hofmann a,b,, Intermetallics 39 (2013) 89e93
[13] K.S. Lee, Yu Mi Jo, Young-Seon Lee, J. Non-Cryst. Solids 376 (2013) 145-151
[14] C.N. Kuo, J.C. Huang, J.B. Li, J.S.C. Jang, C.H. Lin, T.G. Nieh, J. Alloys Compd. 590 (2014) 453-458
[15] Weibing Liao, Yangyong Zhao, Jianping He, Yong Zhang, J. Alloys Compd. 555 (2013) 357-361
[16] B.W. Zhou, X.G. Zhang, W. Zhang, H. Kimura, T. Zhang, A. Makino, A. Inoue, Mater. Transactions, 51 (2010) 826-829
[17] Y.H. Li, W. Zhang, C. Dong, J.B. Qiang, A. Makino, A. Inoue, Intermetallics 18 (2010) 1851.
[18] S.H. Chen, K.C. Chan, L. Xia, Mater. Sci. Eng. A 606 (2014) 196-204
[19] Boer FR, Boom R, Mattens WCM, Miedema AR, Niessen AK, Cohesion and structure. Cohesion in metals, Vol. 1. Amsterdam, Elsevier Science; 1988
[20] D. Wang, H. Tan, Y. Li, Acta Mater. 53 (2005) 2969-2979
[21] G. Kőrösy, K. Tomolya, D. Janovszky, J. Sólyom, Mat. Sci. Forum 729 (2013) 419-423
[22] K. Tomolya, D. Janovszky, A. Sycheva, Mat. Sci. Forum 790-791 (2014) 509-514
[23] Zengqian Liu, Ran Li, Hui Wang, Tao Zhang, Nitrogen-doping effect on glass formation and primary phase selection in Cu–Zr–Al alloys, J. Alloys Compd., 509 (2011) 5033-5037
[24] Xinlin Yan, X.-Q. Chen, A. Grytsiv, P. Rogl, R. Podloucky, V. Pomjakushin, H. Schmidt, G. Giester, Intermetallics 16 (2008) 651-657
[25] H. Bo, J. Wang, S. Jin, H.Y. Qi, X.L. Yuan, L.B. Liu, Z.P. Jin, Intermetallics 18 (2010) 2322-2327